IDENTIFICATION OF BATCH CRYSTALLIZATION CONTROL STRATEGIES USING CHARACTERISTIC CURVES

CHUEI-TIN CHANG

FMC Corporation
Princeton, NJ 08540

and

MARY A. FARRELL EPSTEIN

Trinity College
Hartford, CT 06106

Optimal control studies have been carried out for a batch cooling crystallizer using lumped parameter system equations that describe the dynamic behavior of the leading CSD moments. Various performance indices, all of which can be defined in terms of moments, were used in our studies, e.g., the product number average size, volume, variance and a combination of them. The corresponding operating condition sequences for maximizing (or minimizing) these performance indices were calculated using Kelley's gradient method. An algorithm based on the method of characteristics was developed to recover the corresponding solution surface of the original distributed-parameter population balance equation. The numerical values of the results obtained by the two approaches, i.e., lumped and distributed, were found to be very close. This implies that the suggested algorithm can be used to interpret the CSD transient. Furthermore, it can also be considered as a potential method to estimate the transient CSD on-line.

Few studies have investigated the control strategies of batch crystallization processes (1,2,3). Only one of them was based on the population balance equation (PBE). Jones (1) applied Pontryagin's Maximum Principle (4) to calculate the opitmal cooling curve using the seed size as the performance index and the transformed moment equations as the system governing equations. The product crystal size distribution was then recovered by Laguerre approximation (5) using available leading moments. The approximation, however, does not guarantee a satisfactory result. A more reliable method, i.e., the method of characteristics, is adopted in this study to reconstruct to entire n-y-t (number density-size-time) surface. Furthermore, the seeds' size is not the only performance index that we are interested in optimizing. Several other criteria are proposed here, such as maximizing the average product size or the volume of solid product, to calculate the optimal temperature sequence. Then, the corresponding transient CSD's are recovered using the method of characteristics.

The Maximum Principle allows us to determine only open-loop control policies.

Columbia University, New York, New York. C.-T. Chang is now with FMC Corporation, Princeton, New Jersey. M.A. Farrell Epstein is with Trinity College, Hartford, Connecticut.

0065-8812-82-0000-0215-$2.00

To date, there have been no studies concerned with the closed-loop control of batch crystallization. Although many papers have been published recently for continuous crystallizer control systems (6, 7, 8, 9, 10), on-line measurement and estimation of the CSD are still considered significant problems. For batch crystallization, the method of characteristics requires only the knowledge of number densities at the boundary of y-t plane, which are potentially measurable with available instrumentation. The close agreement between the values obtained from the moment equations and those obtained by the method of characteristics in our studies indicates that the distributed approach can also be considered as a possible estimator for batch crystallizer control systems.

OPTIMUM CONTROL STUDIES

Model Formulation:

For a batch crystallizer, the population balance equation (PBE) can be written as:

$$\frac{\partial n}{\partial t} + \frac{\partial (nG)}{\partial y} = 0 \qquad (1)$$

with boundary conditions:

$$n(0,t,T) = B^{o}(t,T)/G(t,T)$$

and $n(y,0) = n_s(y)$

Using the moment transformation (5, 11), we can change the population balance equation into four ordinary differential equations:

$$\frac{dm_0}{dt} = B^o(m_3, T) \tag{2}$$

$$\frac{dm_1}{dt} = m_0 G(m_3, T)$$

$$\frac{dm_2}{dt} = 2m_1 G(m_3, T)$$

$$\frac{dm_3}{dt} = 3m_2 G(m_3, T)$$

In published literature, the growth rate, G, and the nucleation rate, B^o, are generally considered to be functions of solute concentration (supersaturation), magma density and temperature. However, since the total amount of solute in the batch crystallizer, present both as crystals and as dissolved solute, is constant throughout the operation period, G and B^o can be regarded as functions of temperature and the third moment of the current CSD. Equations (2) can be used as our system governing equations if we are only interested in optimizing performance indices that can be expressed in terms of the moments. Under the condition that the total operation time is fixed, several criteria of optimization have been considered. First, if we are interested in maximizing the average size of the product crystals, the performance index to be minimized will be

$$J_1 = -\left.\frac{m_1}{m_0}\right]_{t_f} \tag{3}$$

Second, the performance index for maximizing the total volume of product crystals is

$$J_2 = -\left.m_3\right]_{t_f} \tag{4}$$

Similarly, the performance index for minimizing the variance and maximizing the number average size of the final CSD at the same time will be

$$J_3 = \left\{ \left[\frac{m_2}{m_0} - \left(\frac{m_1}{m_0} \right)^2 \right] - \alpha \frac{m_1}{m_0} \right\}_{t_f} \tag{5}$$

where α is a weighting factor Furthermore, in practical operation, it may be necessary to consider the deviation between system temperature and some fixed temperature, Tm, which can be easily maintained without control. Thus, the performance indices in Equations (3-5) can be changed to

$$J = J_j + \beta \int_{t_o}^{t_f} (T - T_m)^2 dt \quad , \quad j = 1, 2, 3 \tag{6}$$

where β is also a weighting factor.

THE CONTINUOUS MAXIMUM PRINCIPLE

Having defined the objectives of optimization, we can identify now that the major task is to solve a fixed time Bolza Problem. For completeness, we will briefly describe this problem here in standard notation. Consider the performance index of the form

$$J = K[x(t), t]_{t_f} + \int_{t_o}^{t_f} L[x(t), u(t), t]\, dt \tag{7}$$

subject to a set of arbitrary ordinary differential equations as the system governing equations:

$$\frac{dx}{dt} = f(x, u, t) \tag{8}$$

where K, L and f are arbitrary functionals of the state variables, X(t), manipulated variables, u(t), and time. Applying the Maximum Principle, we can obtain the necessary conditions of minimizing (or maximizing) the performance index, J, with terminal constraints, $N[X(t_f)]$, $t_f = 0$, i.e.,

$$\dot{x} = \frac{\partial H}{\partial \lambda} \tag{9}$$

$$\dot{\lambda} = -\frac{\partial H}{\partial x}$$

$$\delta x \left[\lambda - \frac{\partial K}{\partial x} - \nu \frac{\partial N}{\partial x} \right] = 0 ; \qquad t = t_o, t_f$$

$$\frac{\partial H}{\partial u} = 0$$

where ν is a Lagrange multiplier, λ is the adjoint vector, H is the Hamiltonian, and

$$\lambda \triangleq -L_{\dot{x}} \qquad (10)$$

$$H \triangleq \lambda^T f + L$$

The optimal control problem, therefore, is a problem of finding the manipulated variable, u(t), such that Equations (9) will be satisfied. For our batch crystallizer model, Equations (2) and desired control objectives, Equations (6), the detailed derivation of the adjoint equations and their transversality conditions is straightforward but involved, and, is presented elsewhere (12). There are various techniques available to solve the two point boundary value problem, Equations (9), resulting from the necessary conditions of the Maximum Principle. Kelley's Gradient Method (13) is adopted in our work because it is simple and reliable. A detailed discussion of this algorithm is presented elsewhere(12).

Simulation and Results

Kinetic Data. One of the systems selected for simulation of batch cooling crystallizer operations is KNO_3-water. Kinetic data for growth and nucleation rates have been reported in the literature. The empirical relations reported by Helt and Larson (14) have been adopted for our calculations:

$$G = 4.8\times10^{6}\exp\left[\frac{-31}{R(T+273)}\right]\Delta C \qquad (11)$$

$$B^{\circ}/M_T = 3.0\times10^{-10}\exp\left[\frac{108}{R(T+273)}\right]\Delta C^{1.7}$$

$$\Delta C = C - C_{eq}$$

$$C_{eq} = a_0 + a_1 T + a_2 T^2$$

$$= 0.1362 + 0.00548T + 0.0001752T^2$$

Here, C is the dissolved solute concentration, C_{eq} is the saturated concentration at temperature T and M_T is the magma density. The constants a_o, a_1 and a_2 are determined by regression analysis using data reported in the literature (15).

Initial Conditions. The initial CSD condition chosen for the calculation of optimal temperature profiles can be described by the following uniform distribution:

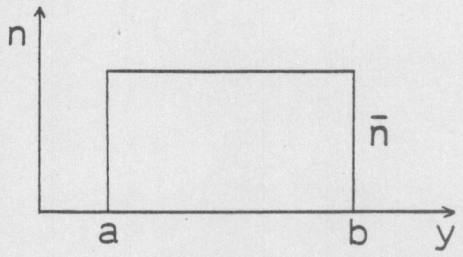

where a=0.0025cm, b=0.0225cm and n=100000#/cm/g H_2O. The first four moments of the above distribution have the following values:

m_o=2000.0
m_1=25.0
m_2=0.3792
m_3=0.006406

For a fixed operation time period, 1000 seconds, all three performance indices proposed earlier have been investigated as criteria for optimization. The fixed temperature, Tm, is arbitrarily chosen to be 42.8°C. Kelley's Gradient Method has been used successfully to search for the extremal location. For J_1 and J_2 five β values ranging from 1.0 to 0.0 are used to study the effect of the weighting factor. For J_3, five β values combined with three α values are adopted to carry out the optimization studies.

Maximizing the Number Average Size of the Final CSD.

From Figure 1, we can see that the final average size is increased when we decrease the weighting factor, β. The effect of weighting factor on temperature can be clearly observed in Figures 2A to 2E, where the deviation of system temperature, T, from Tm increases as β becomes smaller. Examining the corresponding supersaturation profiles in Figures 3A to 3E, we can conclude that it is desirable to create a high supersaturation level at the early stages of operation while keeping supersaturation at a lower level for the remainder of the time. To see how these factors influence the product average size, let's consider the definition of the number average size of the CSD, i.e.,

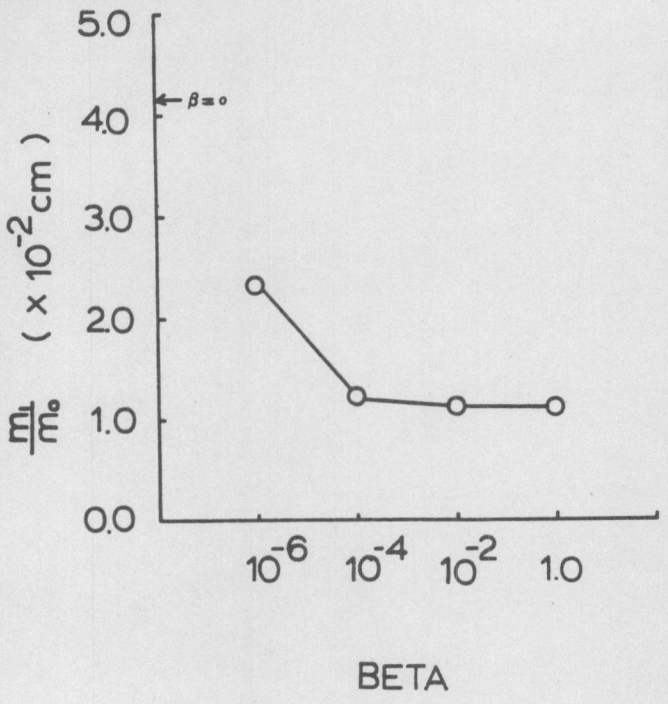

Figure 1. The effect of weighting fact for β on the number average size using performance index J_1.

$$\bar{y} = \frac{m_1}{m_0}\Big]_{t_f} = \frac{1}{m_0(t_f)}\left[\int_{t_o}^{t_f} G(t)\, m_0(t)\, dt + C\right] \tag{12}$$

where

$$\frac{dm_0}{dt} = B^\circ(t) \tag{13}$$

and apply the mean value theorem to Equation (12). Since G(t) is a continuous function of time, Equation (12) can be changed into

$$\bar{y} = \bar{G} \int \phi(t)\, dt + \frac{C}{m_0(t_f)} \tag{14}$$

where $\phi(t) = m_0(t)/m_0(t_f)$ and $0 \leq \phi(t) \leq 1$. Although different supersaturation profiles produce different $\bar{G}$ and $m_0(t_f)$ values, one can be more certain, based on Equation (14), of maximizing the average product size if $\phi(t)$ has a larger initial slope. This will result in a larger initial nucleation rate and, consequently, an increase in the final average size.

Maximizing the Total Volume of the Product Crystals.

The third moment of the CSD, which is a measure of total crystal volume, is

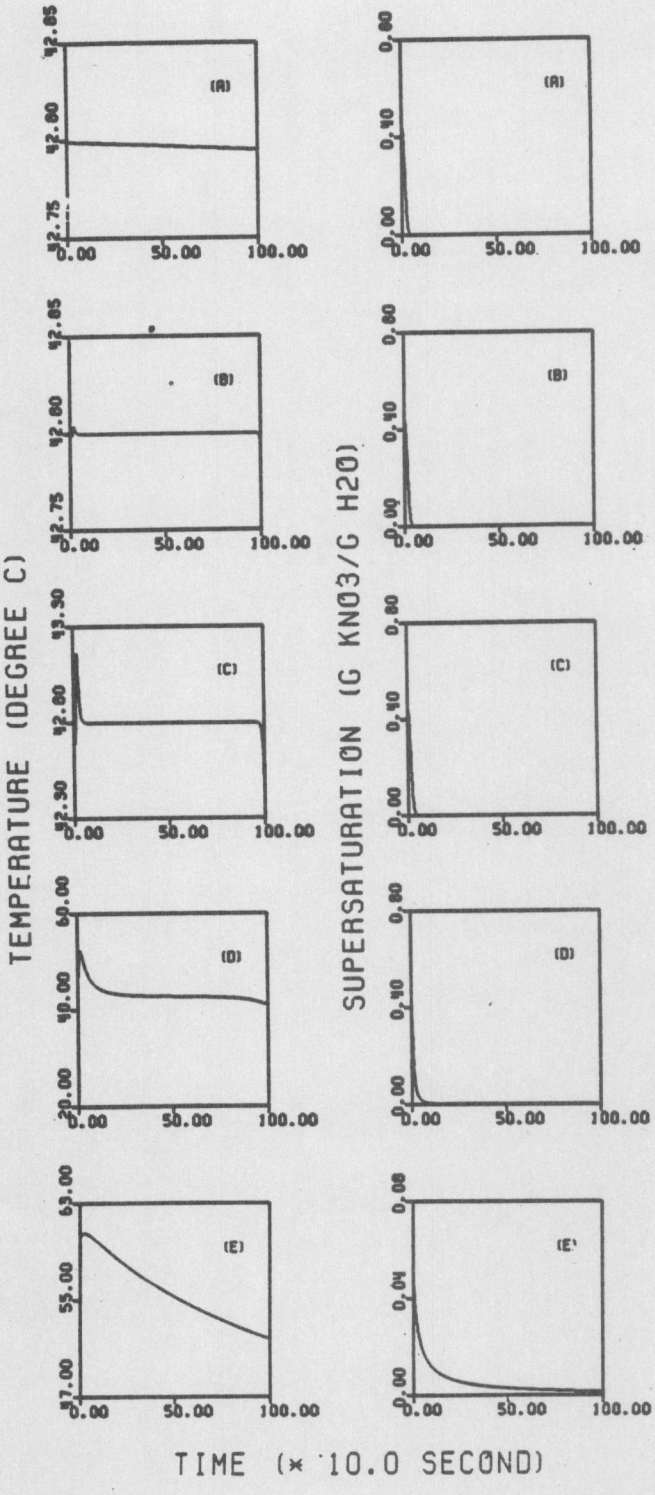

Figure 2. [Left hand column (A) to (E)] Temperature profiles for maximizing the number average size of the final CSD using J_1.

β values: A) 1.0, B) 10^{-2}, C) 10^{-4}, D) 10^{-6}, E) 0.0

Figure 3. [Right hand column (A) to (E)] Supersaturation profiles for the cases shown in Figure 2A to 2E.

increased as the weighting factor, β, is decreased. The corresponding temperature profiles indicate that smaller weighting factors give larger deviations of operating temperature from the fixed temperature, Tm. An initial pulse of supersaturation is observed in all cases, and generates a burst of nuclei. Later, supersaturation is kept at a lower level to allow these nuclei to grow steadily while the nucleation rate is at a low level. For cases with non-zero weighting factor, the sudden drop of temperature at the end is caused by the competition of the two terms in the performance index. For the same squared temperature difference in Equation (6), it is better to drop the temperature at the end because by then a larger crystal surface area has been built up. Thus, more dissolved solute can be deposited on the solid phase (increasing m_3), and the value of performance index will be decreased.

Minimizing the Variance and Maximizing the Number Average Size of the Final CSD: From Figures 4A and 4B, we can observe that (i) the variance is decreased when α and/or β is decreased. However, the effect of β on variance is not conclusive when $\alpha = 1$. (ii) The number average size is decreased when α is decreased, but increased when β is decreased. However, the effect of β on the number average size is not conclusive when $\alpha = 0.0001$.

The exception in (i) is probably due to the fact that the number average size term and the temperature square term in the performance index dominate when $\alpha = 1$, and thus make the variance term relatively unimportant. Similarly, the exception in (ii) occurs because the number average size term is relatively unimportant when $\alpha = 0.0001$.

DISCUSSION

It is interesting to compare our results with the only paper concerning a "size-optimal" control policy for a batch crystallizer, (1). In this paper, Jones predicted that there should be a supersaturation "peak" toward the end of the operation: the reverse of our conclusion. By further examination, we can identify the difference between these two studies: First, the performance index he used is the seeds' size but not the product number average size. Second, the improvement in weight mean size which he mentioned in Table 4 of his paper does not necessarily imply maximization of the product number average size. Keeping the supersaturation low throughout the crystallization period except for a peak at the end allows the seeds to

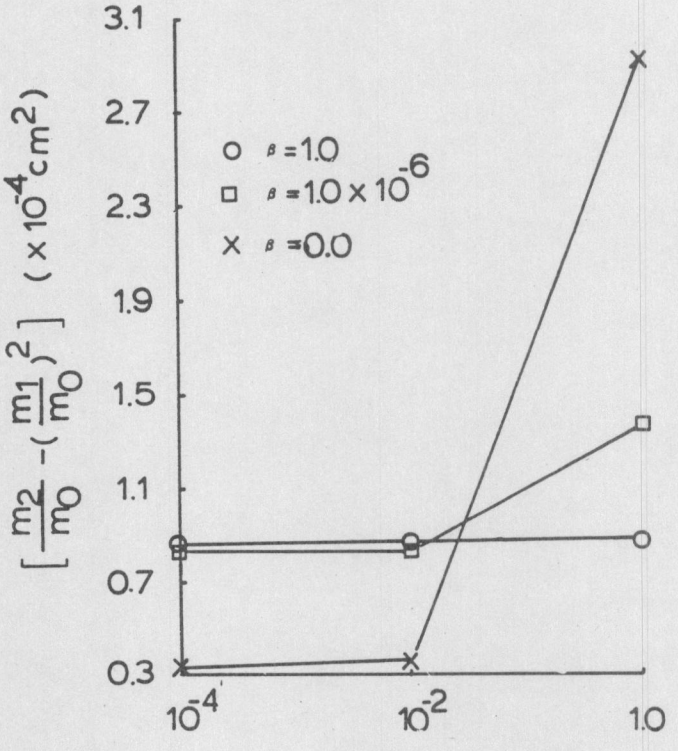

Figure 4A

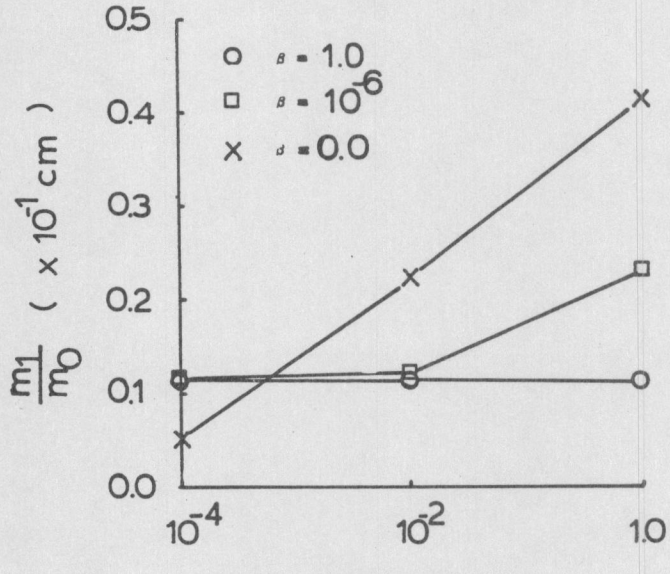

Figure 4B

Figure 4. The effect of weighting factors α and β using performance index J_3 on A) the CSD variance, B) the number average size.

grow steadily for the most of the operation time and to increase in size very rapidly at the end. However, because of secondary nucleation, a huge number of tiny nuclei should also be generated just before ending the operation. Therefore, the final number average size of the resulting CSD will be reduced.

The maximum cooling rate that Jones'experimental equipment could achieve was reported to be 0.042°C/sec. From a practical point of view, it is also useful to evaluate the gradients of the temperature profiles calculated in the present study. The temperature profiles based on the two performance indices, J_1 and J_2, are used as examples here. This is simply because the form of these performance indices is similar to that of the seeds' size. For the optimal temperature sequences calculated for J_1 and J_2, the absolute values of the maximum temperature gradients and the periods of operation when the absolute value of the temperature gradient exceeded 0.042°C/sec were found. These are summarized in Table I. Generally, it can be concluded that the temperature sequences for maximizing the product number average size, J_1's, are more realizable in practice than those for maximizing the product volume, J_2's.

An interpretation in Terms of Characteristic Curves

Using the moment transformation, we changed the population balance equation into a set of ordinary differential equations to which Pontryagin's Maximum Principle was applied. Although certain control criteria have been achieved, e.g., maximum product average size, maximum product volume, etc., the actual transient CSD is still unknown. Therefore, it is very interesting to reconstruct the entire n-y-t surface and obtain a better understanding of crystallization dynamics.

There are various numerical techniques for solving partial differential equations. The algorithm that we have developed is based on the method of characteristics (12).

Using the same initial conditions and the temperature profile calculated by the Maximum Principle, the previous cases for optimizing J_1, J_2 and J_3 have all been tested with this algorithm. For each case, the corresponding final CSD and base characteristic curve, where the base characteristic curve is defined as the curve started from y = 0 at t = 0, were recovered. Figures 5 and 6 show the final CSDs and base characteristic curves for maximizing the number average size (optimizing J_1) for the five β values studied previously. By integrating numerically over the final CSDs (Figure 5) for the corresponding cases presented in Figure 2, we obtained the first four CSD moments. Comparison of these moment values, obtained by our distributed system approach using the method of characteristics, with those obtained by solution of the original moment equations (Equations 2) indicated agreement within 0.5 percent. For objective functions J_2 and J_3, agreement between moments calculated by the distributed system approach with those obtained directly from the moment equations was within 2 percent. This result gave us confidence for interpretation of system

Table 1. Maximum temperature gradients for performance indices J_1 and J_2.

PERFORMANCE INDEX	β	Sm*	$\bar{t}$**
J_1	1.0	0.2289×10^{-4}	0
	1.0×10^{-2}	0.6332×10^{-3}	0
	1.0×10^{-4}	0.6158×10^{-1}	4
	1.0×10^{-6}	0.7043×10^{1}	40
	0.0	0.5685×10^{-1}	2
J_2	1.0	0.2899×10^{-3}	0
	1.0×10^{-2}	0.2802×10^{-1}	0
	1.0×10^{-4}	0.9358	42
	1.0×10^{-6}	0.1134×10^{2}	44
	0.0	0.2475×10^{2}	34

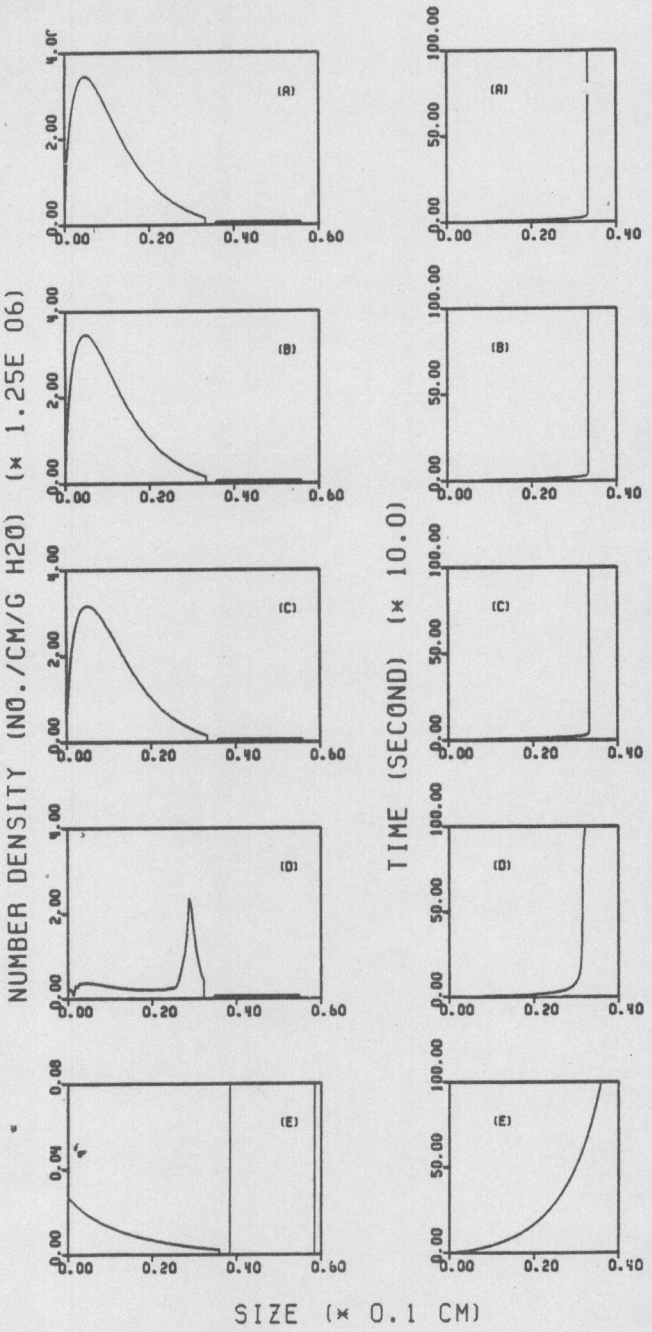

Figure 5. [Left hand column (A) to (E)] Final CSDs for maximizing the number average size corresponding to the temperature profiles of Figures 2A to 2E and supersaturation profiles of Figures 3A to 3E.

Figure 6. [Right hand column (A) to (E)] Base characteristic curves for maximizing the number average size corresponding to the final CSDs in Figures 5A to 5E.

dynamics in terms of characteristic curves. From Figures 5A to 5E, we see that the number average size of the final CSD moves gradually to the right as the weighting factor, β, decreases. Also, the shape of the CSD is changing from skew-to-the-right to skew-to-the-left. From Figures 6A to 6E, we can see that the growth rate, i.e., the reciprocal of the slope of the characteristic curve, decreases more smoothly for a smaller weighting factor than for a larger one.

The method of characteristics also permits recovering of the transient CSD. As an example, the transient behavior of the CSD for maximizing the number average size, with β equal to $1.0 * 10^{-6}$ (Figure 2D), during the first twenty seconds of batch operation is presented in Figure (7).

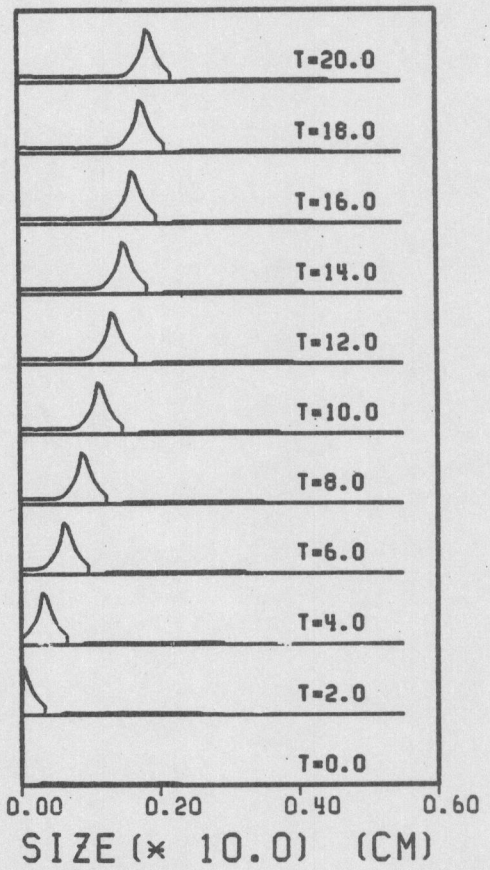

Figure 7. Transient CSD recovered by the method of characteristics for the first 20 seconds of batch operation corresponding to temperature profile of Figure 2D.

CONCLUSION

An optimal control study using the CSD moment equations has been carried out for the batch crystallization processes for different objective functions. The method

of characteristics was used to reconstruct the transient behavior of the CSD for the corresponding cases, and the numerical values of the resulting moments obtained by the two different approaches were in good agreement. This implies that the method of characteristics provides an alternative way to interpret crystallization dynamics for batch systems and can possibly serve as an on-line CSD estimator when implemented with appropriate instrumentation.

Nomenclature:

a_o, a_1, a_2= constants of the solubility curve
B^o= the nucleation rate, #/sec/g H20
C= concentration of dissolved solute, g/g H20
ΔC= supersaturation, g/g H20
G= the growth rate, cm/sec
H= Hamiltonian
J= the performance index
m_o= the zeroth moment of CSD, #/g H20
m_1= the first moment of CSD, cm/g H20
m_2= the second moment of CSD, cm^2/g H20
m_3= the third moment of CSD, cm^3/g H20
M_T= magma density, g/g H20
n= number density, #/cm/g H20
N= terminal constraint
S_m= the absolute value of the maximum temperature gradient, °C/sec
$\bar{t}$= the period of operation when the absolute value of temperature gradient exceeds 0.042°C/sec, sec
t= time, sec
T= temperature, °C
u= the manipulated variable
w_t= total weight of solute, g/g H20
X= the state variable
y= size of the crystals, cm

Greek Letters
α = weighting factor
β = weighting factor
λ = adjoint variable
ν = Lagrange multiplier

Subscripts
f= final stage
0= initial stage
s= seeds
eq= equilibrium

LITERATURE CITED:

1. Jones, A. G., Chem. Eng. Sci., 29, 1075(1974).

2. Jones, A. G. and J. W. Mullin, Chem. Eng. Sci., 29, 105(1974).

3. Mullin, J. W. and J. Nyvlt, Chem. Eng. Sci., 26, 369(1971).

4. Pontryagin, L. S., V. G. Boltyanski, R. V. Gankredize and E. F. Mischenko, The Mathematical Theory of Optimal Processes, English Edition, Interscience, New York(1962).

5. Hulburt, H.M. and S. Katz, Chem. Eng. Sci., 19, 555(1964).

6. Parks, R. M. and R. W. Rousseau, JACC, 819(1979).

7. Randolph, A.D., AIChE Symp. Ser., 76, 1(1980).

8. Randolph, A. D. and G. W. Drach, J. of Crystal Growth, 53, 195(1981).

9. Rovang, R. D. and A. D. Randolph, AIChE Symp. Ser., 76, 18(1980).

10. Shadman, F. and A. D. Randolph, AIChE J., 24, 782(1978).

11. Randolph, A. D. and M. A. Larson, AIChE J., 8, 639(1962).

12. Chang, C.-T., "Control Strategies for Batch Crystallization Processes." PhD. Thesis, Columbia University, New York (1982).

13. Kelley, H. J., "Method of Gradients," in Optimization Techniques, G. Leitman ed., Academic Press, New York(1962).

14. Helt, J. E. and M. A. Larson, AIChE J., 23, 822(1977).

15. Perry, R. H. and G. H. Chilton, "Chemical Engineers' Handbook," 5th Edition, McGraw-Hill Book Company, New York(1973).

16. Randolph, A. D., E. T. White and C.-C. D. Low, Ind. Eng. Chem. Proc. Des. Develop., 20, 496(1981).